Robust depth imaging in adverse scenarios using single-photon Lidar and beta-divergences

Q. Legros*, S. McLaughlin, Y. Altmann
School of Engineering and Physical Sciences
Heriot-Watt University
Edinburgh, United Kingdom
qll1@hw.ac.uk

S. Meignen
Laboratoire Jean Kuntzmann
University Grenoble Alpes
Grenoble, France

Mike E. Davies
School of Engineering
University of Edinburgh
Edinburgh, United Kingdom

***Abstract*—This paper addresses the problem of robust estimation of range profiles from single-photon Lidar waveforms associated with single surfaces using a simple model. In contrast to existing methods explicitly modeling nuisance photon detection events, the observation model considered neglects such events and the depth parameters are instead estimated using a cost function which is robust to model mismatch. More precisely, the family of β-divergences is considered instead of the classical likelihood function. This reformulation allows the weights of the observations to be balanced depending on the amount of robustness required. The performance of our approach is assessed through a series of experiments using synthetic data under different observation scenarios. The obtained results demonstrate a significant improvement of the robustness of the estimation compared to state-of-the-art pixelwise methods, for different background illumination and imaging scenarios.**

***Index Terms*—3D reconstruction, Single-photon lidar, Robust estimation.**

I. Introduction

Light detection and ranging (Lidar) systems have received an increasing interest in the past few years for their ability to efficiently reconstruct 3D scenes at high resolution [1], [2]. One particular case is single photon Lidar (SPL) that uses a high repetition rate pulsed laser source in conjunction with single-photon detectors. One of the main advantages of this technology is its temporal resolution allowing sub-millimeter depth estimation, which makes SPL particularly attractive for a variety of problems such as long range imaging [3], [4], [5], underwater imaging [6], [7], or even through obscurants [8]. Lidar technologies allow the acquisition of the depth structure of scenes, by analysing at the time-of-flight (ToF) of photons originally emitted by a laser source and reflected by surfaces of interest. More precisely, time correlated single-photon counting (TCSPC), which is used in SPL, correlates the time-of-arrivals (ToAs) of detected photons with the time of emission of the last pulse, and often produces ToA histograms. Repeating this acquisition process for different pulse emission directions allows a region of the 3D space to be sensed and reconstructed. However, additional detection events occur in the presence of strongly scattering media and additional light sources, such as solar illumination. Although these events are generally modelled as uniformly distributed, they can present more complex distributions. This is typically the case for instance when imaging through obscurants, where light scattering can produce a significant number of detection events shortly after the pulse emission (photons are reflected with high probability before they can reach the scene of interest).

Bayesian approaches have demonstrated their efficiency to perform a depth profile estimation of the illuminated scene from the Lidar measurements in many different applications [9], [10], [11], [12]. However, the quality of the estimates depends on that of the likelihood (or observation model) used. In this paper, we specifically concentrate on the choice/design of this data fidelity term. Traditionally in SPL analysis, studies have introduced complex parametric models to approximate as accurately as possible the actual data acquisition process, including background illumination, broadening of the system impulse response [13], attenuation due to scattering [14] and detector dead-time [15], [16], [17]. However, such models often comes with an increased computational complexity of the depth estimation process, e.g. can require iterative algorithms.

In this work a simple observation model is considered, whereby we assume that only signal photons, those originally omitted by the laser source, can be detected. The main focus of this work is to estimate the distance between the imaging system and the scene. Although intensity information can be important, it is not addressed here. To overcome the limitations of the simple model used, we do not adopt a maximum likelihood approach but instead use β-divergences [18], [19] to define a more robust depth estimators. Using this family of divergences, we can reinterpret the classical depth estimator via matched filtering (MF), seen as a specific minimum divergence depth estimator for SPL. Using β-divergences for SPL has been recently investigated, in a pseudo Bayesian framework in [20], where the main focus was to propose an online 3D imaging method. Here, we do not adopt a Bayesian perspective and concentrate on pixelwise, regularization-free depth estimation, to better understand the benefits of the β-divergence in various illumination conditions and several types

This work was supported by the Royal Academy of Engineering under the Research Fellowship scheme RF201617/16/31, the UK Defence Science and Technology Laboratory (DSTL X1000114765) and by the Engineering and Physical Sciences Research Council (EPSRC) (grants EP/N003446/1, EP/T00097X/1 and EP/S000631/1) and the MOD University Defence Research Collaboration (UDRC) in Signal Processing. M. D. acknowledges support from the Royal Society Wolfson Research Merit Award and the ERC advanced grant C-SENSE, project 694888.

of model mismatch.

The remainder of this paper is organized as follows. Section II introduces and motivates the simple observation model considered in this study. The divergence used for robust depth estimation in the presence of an imperfectly known system impulse response function (IRF) is introduced in Section III. A comparison to state-of-the-art approaches using synthetic data is conducted in Section IV to identify benefits of the proposed approach. Conclusions are finally reported in Section V.

II. Observation model

In this paper, we address the pixelwise estimation of object range from SPL data. Thus, to simplify notation, we omit indices representing pixel dependency. Two main pixelwise representations of photon ToAs are currently used in the context of SPL. The earliest methods have considered each pixel as a ToA histogram $\boldsymbol{y} = [y_1, \dots, y_T]^\top$, which consists of T non-overlapping temporal bins (the bin width being usually given by the temporal resolution of the detector). Note that in this work, we implicitly assume that the repetition period of the laser source is T, where the arbitrary time unit is width of a temporal bin. However, with the development of high-resolution photodetectors, T can be extremely large (although the actual temporal span of the histogram remains constant, the width of the time bins decreases) and the measured ToAs can now also be seen as continuous variables [5]. In a context of photon-starved measurements, the alternative ToA representation is simply based on sets of individual photon ToAs. If we assume that P photons are detected, the observations are denoted by $\boldsymbol{s} = \{s^p\}_{p=1}^P$, where s^p is the ToA of the pth detected photon.

Neglecting detector dark counts and additional light sources apart from the classical emission laser and assuming the a single surface is visible in the field of view, the observation model for any ToA s can be expressed as

$$f(s|d) = h\left(s - \frac{2d}{c}\right), \tag{1}$$

where h is the normalized IRF associated with the imaging system. This IRF is generally measured during calibration of the Lidar-based imaging system. In (1), c is the speed of light and d is the distance to the target, such that $\frac{2d}{c}$ is the characteristic ToF associated with the illuminated target. Eq. (1) implicitly assumes that the scene is approximately static and that the shape of $h(\cdot)$ remains the same for all the admissible values of d. When P photons are detected, if the dead-time of the detector can be neglected, the photon ToAs are mutually independent (given d) and the joint likelihood can be expressed as

$$f(\boldsymbol{s}|d) = \prod_{p=1}^{P} f(s^p|d). \tag{2}$$

III. Robust estimation using β divergences

The model in (2) is simple (it only depends on a single parameter d per pixel) but is often not accurate enough, especially when ambient illumination cannot be neglected. In particular, using maximum likelihood (ML) estimation strategies using Eq. (1) to infer d yields poor estimation performance.

In general, the observation model used for depth estimation is chosen to be "similar" to the actual (to usually unknown) data distribution, to enable reliable parameter estimation. The similarity measure used also impacts the estimation performance. For instance, the estimator constructed from the ML criterion can also by seen as the estimator minimizing the Kullback-Leibler (KL) divergence $\mathrm{KL}(\hat{g}(s)||f(s|d))$, between the empirical data distribution $\hat{g}(s) = \frac{1}{P}\sum_{p=1}^{P}\delta(s - s^p)$ and the postulated observation model in (1) ($\delta(\cdot)$ stands for the Dirac delta function). Instead of using the traditional KL as similarity measure, here we consider a more general family of divergences, to reflect the potential mismatch between the actual data distribution and the postulated model. The main objective here is to use a similarity measure that leads to a robust and computationally attractive depth estimator, where *robust* refers to the presence of spurious detection events.

In this work, we consider the family of β-divergences, defined by

$$\begin{aligned}\mathrm{D}_\beta(g||f) = \int_0^T & f^{1+\beta}(x|d) - \frac{1+\beta}{\beta}\left[g(x)f^\beta(x|d)\right] \\ & + \frac{1}{\beta}\left[(g)^{1+\beta}(x)\right]\mathrm{d}x, \quad \beta > 0.\end{aligned} \tag{3}$$

to measure the similarity between two distributions g and f. In a similar fashion to the ML estimation which reduces to minimizing $\mathrm{KL}(\hat{g}(s)||f(s|d))$, here we estimate the depth in (1) by minimizing $\mathrm{D}_\beta(\hat{g}(s)||f(s|d))$. Under mild assumptions, the resulting estimator is given

$$\hat{d} = \underset{d}{\operatorname{argmax}} \quad \left\{\frac{1+\beta}{\beta P}\sum_{p=1}^{P} f^\beta(s^p|d) - \text{Const.}\right\}, \tag{4}$$

where the constant corresponds to the first and third terms on the right-hand side of Eq. (3). While the third term does not depend on d, the first term does not either in practice as we assume that the shape and the integral of $h(\cdot)$ does not depend on d over its domain of definition ($2d/c$ is expected to be far from 0 and T). Note that $f^{1+\beta}(x|d)$ depends on divergence parameter β though.

An interesting link with histogram-based depth estimation methods and (4) has been discussed in [20] and is briefly recalled here. If the data in $\boldsymbol{s}$ are represented using $\boldsymbol{y}$, i.e., a set photons counts being detected in each of the T time bins, Eq. (4) can be rewritten

$$\hat{d} = \underset{d}{\operatorname{argmax}} \quad \sum_{t=1}^{T} y_t h^\beta\left(t - \frac{2d}{c}\right), \tag{5}$$

which corresponds to maximizing the cross-correlation between $\left[h^\beta\left(1 - \frac{2d}{c}\right), \dots, h^\beta\left(T - \frac{2d}{c}\right)\right]^\top$ and $\boldsymbol{y}$.

The depth estimation based on (5) (or (4)) depends on the divergence parameter β. Two special cases to be mentioned are

1) when $\beta = 1$, where solving Eq. (5) reduces to matched-filtering the data with $h^{\beta}(t - \frac{2d}{c})$, and 2) when $\beta \to 0$, where solving Eq. (5) reduces to log-matched filtering the data with the logarithm of $h(t - \frac{2d}{c})$. In the latter case, the resulting estimator is the classical ML estimator (the β-divergence converges to the KL divergence when $\beta \to 0$).

Solving Eq. (4) instead of maximizing the classical log-likelihood leads to a pseudo-ML estimation, also referred to as minimum divergence (MD) estimation.

IV. Results

In this section, we assess the depth reconstruction performance of the proposed approach by comparing it to that of existing pixelwise estimation procedures. We first consider two IRFs, (depicted in Fig.1 top), i.e., a real asymmetric IRF measured in [21] and a Gaussian IRF presenting the same full width at half maximum (FWHM) (28 bins, each bin representing a 2ps interval) and the same mode. Based on these IRFs, we generated synthetic data with $T = 1500$ and added different types of model mismatch, including constant and non-uniform background levels and measured peaks broader than the original IRF, referred to as IRF broadening, as typically occurs when the surface imaged is not orthogonal to the beam direction [13]. For all the methods considered, we set the admissible temporal range to $[t_{min}, t_{max}] = [101, 1400]$, which ensures that the integrals of the IRFs remain constant over the admissible object range. All the results presented have been averaged over $N_{iter} = 2000$ Monte Carlo realizations. Different scenarios have been reproduced to assess the performance of the proposed method through both the mean signal photon counts (MSC) and the average signal to background ratio (SBR). The MSC is the number of detected photons originally emitted by the laser and whose distribution is given by (1), and the SBR is defined as the ratio of the MSC over the total number of nuisance detection events. For each scenario, data have been simulated using different MSCs, ranging from 1 to 10^3 and SBRs between 10^2 and 10^{-4}, with the ground truth depth fixed to correspond to the 620th bin.

Our method is compared to ML and robust estimators for pixelwise depth estimation. More precisely, we considered the log-matched filtering (LMF) approach, which is the ML estimator based on Eq. (2), the robust Huber's estimator [22], [23], the Half-sample-mode (HSM) estimator [24]. For all the simulations, we also considered the Oracle estimator, i.e., the ML estimator of the depth based on the true model used to generate the data, with other model parameters (e.g. SBR and MSC) being set to their actual values. Note that Huber's estimator requires a user-defined hyperparameter to be tuned, and it has been fixed to 0.4 for the experiments conducted in this work, aiming to discard 80% of the detected photons prior to estimating the truncated mean with the remaining data. This value has been set such that the performance of the estimator remains satisfactory across a range of SBR values.

To quantify the depth estimation quality, we computed the probability of *accurately* estimating the target depth, whereby a detection is deemed accurate if the absolute error between the estimated depth and the ground truth is below a threshold that has been fixed to the IRF FWHM. The curves displayed in Fig. 2 represent for each SBR the MSC necessary to reach a probability of accurate detection higher than 85% (the working region of each method is on the right-hand side of each curve).

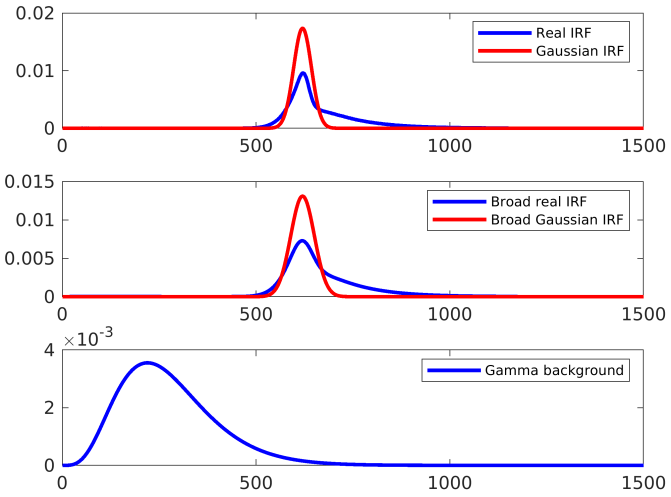

Fig. 1. Top: Real asymmetric (red) and Gaussian IRFs used to simulate the data used for the experiments in Sections IV-A and IV-C. Middle: broadened IRFs used in Section IV-B, obtained by convolving the IRFs from the top plot with a Gaussian of standard deviation 20. Bottom: gamma distribution used to generate non-uniform background detection events in Section IV-C.

A. Constant background level

In this section, we first investigate the robustness of the selected methods, in the case of constant background levels corrupting the observations. The main results are presented in Fig. 2.

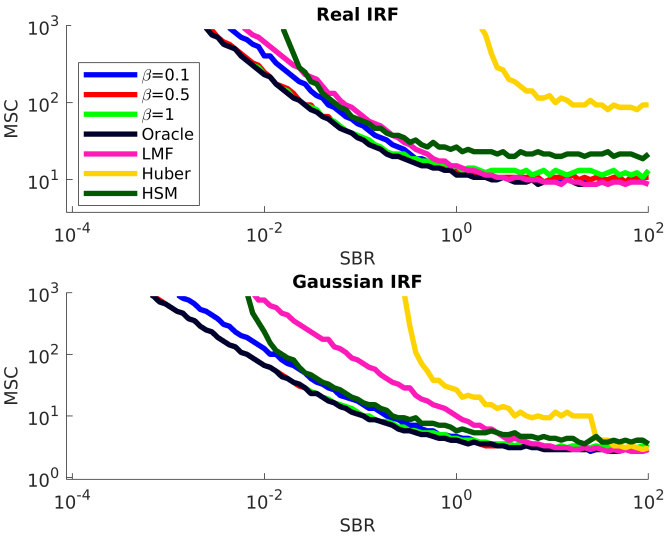

Fig. 2. Threshold of accurate detection higher than 85% for different robust methods, as function of the MSC and SBR. Top: results related to data generated with the real IRF displayed in red in Fig. 1top. Bottom : histograms generated with the Gaussian IRF approximation displayed in blue in Fig. 1 top.

Note first in Fig. 2 that using the real IRF (top) or its Gaussian approximation (bottom) does not modify the order of performances of the compared methods. Although the IRF shape does not seem to affect the relative performance of the methods considered, it impacts the overall performance as show in Fig. 2 (bottom) where the symmetry of the IRF seems to improve the estimation performance. The best estimation performance is obtained by the proposed MD for β close to 1, whereas the worst estimation is obtained with Huber. The performance of the MD is significantly improved when β is increased, but this tails off when β gets closer to 1. The detection threshold associated with the MD estimators converge to that of the Oracle when β tends to 1. Even though high values of β enhance the depth estimation performance for low SBR cases, we observe the opposite phenomena when the SBR is higher than 1. HSM gives on average worse performance than MD, but performs better than Huber.

B. Broadening of the IRF

In this section, we assess the performance of our method in situations where the empirical IRF is broader than the postulated IRF (see Fig. 1 middle). IRF broadening can occur when surfaces observed that are not orthogonal to direction of the laser beam and when the size of the laser footprint on target can no longer be neglected. It can also occur in the presence of partially transparent materials, whereby part of the light penetrates deeper into the objects before being reflected (e.g. forest canopy). For simplicity, the broadened IRFs (see Fig. 1 middle) are modeled here by convolving the true IRFs from Fig. 1 top) by a Gaussian kernel whose standard is equal 20 bins.

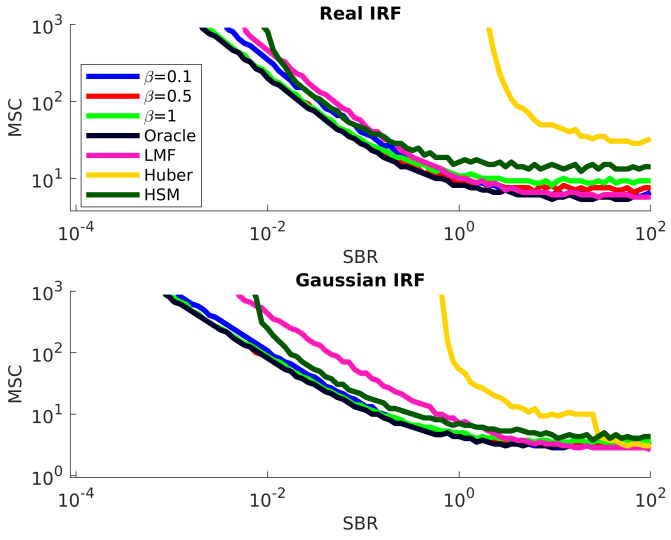

Fig. 3. Threshold of accurate detection higher than 85% for different robust methods, as function of the MSC and SBR. Top : results obtained with a broad version of the real IRF displayed in red in Fig. 1top. Bottom : results obtained with a broad version of the Gaussian IRF displayed in blue in Fig. 1top.

The main results obtained with broadened IRFs are depicted in Fig. 3. This figure shows that the estimation performance of the MD estimators and the LMF remain similarly to that depicted in Fig. 2. The best performance is still obtained by the Oracle that gives the SBR bound (for a given MSC) under which all the other methods provide less than 85% of accurate detection. The MD estimator for high values of β provides the most robust reconstructions whereas Huber provides the least satisfying ones (still relative to the fixed detection threshold). HSM achieves similar performance than in Fig. 2, and is less robust than the MD estimators. As in Fig. 2, the symmetry of the IRF used in Fig. 3 (bottom) enhances slightly the estimation performance of all the methods. However, the Huber estimator seems more affected by the asymmetry of the IRF (Fig. 3 (top)).

C. Non-uniform background

Imaging scenarios in presence of scattering media are receiving growing interest in underwater and automotive (e.g. fog and rain) applications. In such cases, the background temporal profile is expected to follow a non-uniform distribution. To investigate this issue, we applied our method to data generated with a gamma background distribution, depicted in Fig. 1 (bottom). The parameters of the gamma distribution have been set to 5 bins (shape) and 55 bins (scale) and this profile is similar to that observed in [7].

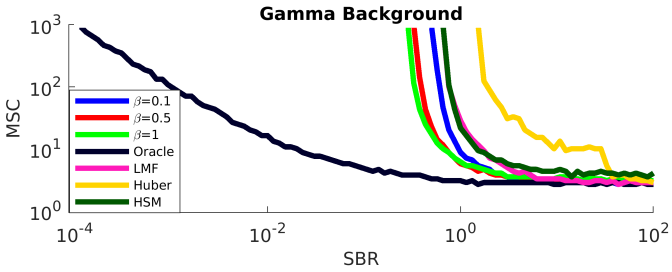

Fig. 4. Threshold of accurate detection higher than 85% for different robust methods, as function of the MSC and SBR. The outliers corresponds to background photons following a gamma distribution, and the Gaussian IRF (see Fig. 1 top) has been used to generate and analyze the data.

The estimation performance of the different methods is assessed in Fig. 4. As in Figs. 2 and 3, the MD method provides better results as β increases. The worst estimation are obtained with Huber and HSM performs similarly than LMF in this case. Note that here, the Oracle performs significantly better than in Fig. 2, due to the non-uniform nature of the noise. While the proposed method can mitigate the presence of uniform background and IRF broadening, its gain here is more limited. Consequently, using a parametric model (which accounts for the shape of the background distribution) is more adapted.

D. Computational complexity

The two pixelwise representations of the photon ToAs introduced in Section II (involving $\mathbf{y}$ or $\mathbf{s}$) play a key role in the complexity of the proposed estimator. Although the use of $\mathbf{y}$ allows us to retrieve the matched filtering formulation, the best ToA representation is still user/scenario dependent. While

the evaluation of the cost function in (5) depends linearly on the number of (non-empty) histogram bins in $\boldsymbol{y}$, which is at most T, the evaluation of the cost function in (4) depends on the number of detected photons P (assuming they all have different ToAs). Thus, the most suited representation will depend on the amount of ToAs acquired.

The quantitative comparison of the different methods used in this paper in terms of computational complexity is not included here as the complexity can be highly platform (sequential of parallel) and implementation dependent. Nonetheless, it is possible to qualitatively compare their complexity. The proposed robust method has roughly the same computational cost as the standard LMF as it reduces to computing a similar cross-correlation (LMF uses $\log(f(\cdot))$ while MD uses $f^{\beta}(\cdot)$). Huber is generally faster than MD and LMF for low photon counts, but is not well adapted to thousands of photon counts. Finally, HSM relies on an iterative algorithm whose number of iterations grows with the number of photons and is not adapted to large photon counts either (it becomes rapidly slower than Huber and MD/LMF).

V. Conclusion

In this paper, we proposed a new depth estimator for robust estimation of the range profile from single-photon Lidar data, in the presence of non negligible background. The proposed formulation of the problem significantly simplifies the estimation process as it relies on the estimation of a single parameter, i.e., the depth parameter. To alleviate the robustness issues of the classical maximum likelihood approach, β-divergences are used instead of the Kullback-Leibler divergence to quantify the similarity between the empirical data distribution and the postulated distribution. We compared the estimation performance of the proposed estimator to that of existing pixelwise approaches for different observation scenarios, and demonstrated its potential benefits over the classical pixelwise log-matched filter. Moreover, the estimation process benefits from a low complexity, similar to that of log-matched filtering. Beyond pixelwise estimation, such a robust estimation strategy can be coupled, as in [20], with prior/regularization terms to further enhance the estimation performance. However, using such β-divergences within a Bayesian framework requires further investigation to better understand and balance the relative weights of the data fidelity and regularization terms. Future work include the consideration of alternative families of divergences or similarity measures. Moreover, it would also be interesting to investigate if such robust methods could be used to mitigate dead-time detector limitations [16], [17].

References

[1] T. Bosch, "Laser ranging: a critical review of usual techniques for distance measurement," *Opt. Eng.*, vol. 40, no. 1, 2001.

[2] P. Vines, K. Kuzmenko, J. Kirdoda, D. Dumas, M. Mirza, R. Millar, D. Paul, and G. Buller, "High performance planar ge-on-si single-photon avalanche diode detectors," *Nature Communications*, Sept. 2018.

[3] A. M. Pawlikowska, A. Halimi, R. A. Lamb, and G. S. Buller, "Single-photon three-dimensional imaging at up to 10 kilometers range," *Opt. Express*, vol. 25, no. 10, pp. 11 919–11 931, May 2017.

[4] Z.-P. Li, X. Huang, Y. Cao, B. Wang, Y.-H. Li, W. Jin, C. Yu, J. Zhang, Q. Zhang, C.-Z. Peng, F. Xu, and J.-W. Pan, "Single-photon computational 3D imaging at 45 km," 2019.

[5] Z.-P. Li, X. Huang, P.-Y. Jiang, Y. Hong, C. Yu, Y. Cao, J. Zhang, F. Xu, and J.-W. Pan, "Super-resolution single-photon imaging at 8.2 kilometers," *Opt. Express*, vol. 28, no. 3, pp. 4076–4087, 2020.

[6] A. Maccarone, A. McCarthy, X. Ren, R. E. Warburton, A. M. Wallace, J. Moffat, Y. Petillot, and G. S. Buller, "Underwater depth imaging using time-correlated single-photon counting," *Opt. Express*, vol. 23, no. 26, pp. 33 911–33 926, 2015.

[7] A. Maccarone, F. M. Della Rocca, A. McCarthy, R. Henderson, and G. S. Buller, "Three-dimensional imaging of stationary and moving targets in turbid underwater environments using a single-photon detector array," *Opt. Express*, vol. 27, no. 20, pp. 28 437–28 456, 2019.

[8] R. Tobin, A. Halimi, A. McCarthy, M. Laurenzis, F. Christnacher, and G. S. Buller, "Three-dimensional single-photon imaging through obscurants," *Opt. Express*, vol. 27, no. 4, pp. 4590–4611, Feb. 2019.

[9] R. Tobin, Y. Altmann, X. Ren, A. McCarthy, R. A. Lamb, S. McLaughlin, and G. S. Buller, "Comparative study of sampling strategies for sparse photon multispectral Lidar imaging: towards mosaic filter arrays," *Journal of Optics*, vol. 19, no. 9, p. 094006, Aug. 2017.

[10] Y. Altmann, A. Wallace, and S. McLaughlin, "Spectral unmixing of multispectral Lidar signals," *IEEE Trans. Signal Process.*, vol. 63, no. 20, pp. 5525–5534, Oct. 2015.

[11] J. Tachella, Y. Altmann, M. Márquez, H. Arguello-Fuentes, J.-Y. Tourneret, and S. McLaughlin, "Bayesian 3D reconstruction of subsampled multispectral single-photon Lidar signals," *IEEE Trans. Comput. Imaging*, Aug. 2019.

[12] A. Halimi, R. Tobin, A. McCarthy, J. M. Bioucas-Dias, S. McLaughlin, and G. S. Buller, "Robust restoration of sparse multidimensional single-photon Lidar images," *IEEE Trans. Comput. Imaging*, 2019.

[13] J. Tachella, Y. Altmann, S. McLaughlin, and J. . Tourneret, "3D reconstruction using single-photon lidar data exploiting the widths of the returns," in *Proc. IEEE Int. Conf. Acoust., Speech, and Signal Processing (ICASSP)*, 2019, pp. 7815–7819.

[14] A. Maccarone, A. McCarthy, A. Halimi, J. Tachella, P. S. Chhabra, Y. Altmann, A. M. Wallace, S. MaLaughlin, Y. R. Petillot, and G. S. Buller, "Time-correlated single-photon counting for single and multiple wavelength underwater depth imaging," in *Advanced Photon Counting Techniques XII*, vol. 10659. International Society for Optics and Photonics, 2018, p. 106590R.

[15] A. Gupta, A. Ingle, and M. Gupta, "Asynchronous single-photon 3D imaging," in *Proceedings of the IEEE International Conference on Computer Vision*, 2019, pp. 7909–7918.

[16] A. Gupta, A. Ingle, A. Velten, and M. Gupta, "Photon-flooded single-photon 3D cameras," in *Proceedings of the IEEE Conference on Computer Vision and Pattern Recognition*, 2019, pp. 6770–6779.

[17] J. Rapp, Y. Ma, R. M. Dawson, and V. K. Goyal, "Dead time compensation for high-flux ranging," *IEEE Trans. Signal Process.*, vol. 67, no. 13, pp. 3471–3486, 2019.

[18] F. Futami, I. Sato, and M. Sugiyama, "Variational inference based on robust divergences," in *Intern. Conf. on Artificial Intel. and Stat., AISTATS 2018, 9-11 April 2018, Playa Blanca, Lanzarote, Canary Islands, Spain*, A. J. Storkey and F. Pérez-Cruz, Eds., vol. 84. PMLR, 2018, pp. 813–822.

[19] A. Basu, I. R. Harris, N. L. Hjort, and M. Jones, "Robust and efficient estimation by minimising a density power divergence," *Biometrika*, vol. 85, no. 3, pp. 549–559, 1998.

[20] Q. Legros, J. Tachella, R. Tobin, A. McCarthy, S. Meignen, G. S. Buller, Y. Altmann, S. McLaughlin, and M. E. Davies, "Robust 3D reconstruction of dynamic scenes from single-photon lidar using beta-divergences," April 2020, unpublished.

[21] R. Tobin, Y. Altmann, X. Ren, A. McCarthy, R. A. Lamb, S. McLaughlin, and G. S. Buller, "Comparative study of sampling strategies for sparse photon multispectral lidar imaging: towards mosaic filter arrays," *J. of Optics*, vol. 19, no. 9, p. 094006, aug 2017.

[22] P. J. Huber, "Robust estimation of a location parameter," *Ann. Math. Statist.*, vol. 35, no. 1, pp. 73–101, 03 1964.

[23] R. Wilcox, *Introduction to Robust Estimation and Hypothesis Testing*, ser. Statistical Modeling and Decision Science. Elsevier Science, 2012.

[24] D. R. Bickel and R. Früwirth, "On a fast, robust estimator of the mode: Comparisons to other robust estimators with applications," *Computational Statistics & Data Analysis*, vol. 50, no. 12, pp. 3500 – 3530, 2006.